

Novel aromatase inhibitors selection using induced fit docking and extra precision methods: Potential clinical use in ER-alpha-positive breast cancer

Ranjith Kumavath^{1*}, Manan Azad¹, Pratap Devarapalli¹, Sandeep Tiwari³, Shreya Kar⁴, Debmalya Barh², Vasco Azevedo³ & Alan Prem Kumar⁴⁻⁸

¹Department of Genomic Science, School of Biological Sciences, Central University of Kerala, Padannakad P.O., Kasaragod-671314, Kerala, India; ²Centre for Genomics and Applied Gene Technology, Institute of Integrative Omics and Applied Biotechnology (IIOAB), Nonakuri-721172, PurbaMedinipur, West Bengal, India; ³Instituto de Ciências Biológicas, Universidade Federal de Minas Gerais, MG, Brazil; ⁴Cancer Science Institute of Singapore, National University of Singapore, Singapore-117599; ⁵National University Cancer Institute, National University Health System, Singapore-119074; ⁶Department of Biological Sciences, University of North Texas, Denton-762035017, Texas, USA; ⁷Department of Pharmacology, Yong Loo Lin School of Medicine, National University of Singapore, Singapore-117600; ⁸Faculty of Health Sciences, School of Biomedical Sciences, Curtin University, Bentley, Western Australia-6102; Dr. Ranjith Kumavath - Email: rnkumavath@gmail.com; RNKumavath@cukerala.edu.in; Phone: 0091-8547648620; Fax: 0467-2282250; Dr. Alan Prem Kuma - Email: csiapk@nus.edu.sg; *Corresponding author

Received April 5, 2016; Revised May 25, 2016; Accepted August 12, 2016; Published October 10, 2016

Abstract:

Aromatase (*CYP19A1*) the key enzyme of estrogen biosynthesis, is often deregulated in breast cancer patients. It catalyzes the conversion of androgen to estrogen, thus responsible for production of estrogen in human body. However, it causes over-production of estrogen which eventually leads to proliferation of breast cancer cells. Identification of new small molecule inhibitors targeted against *CYP19A1* therefore, facilitates to increase drug sensitivity of cancer cells. In this scenario, the present study aims to identify new molecules which could block or suppress the activity of aromatase enzyme by molecular docking studies using Schrödinger-Maestro v9.3. In this study we used *in silico* approach by modeling *CYP19A1* protein the structure was subjected to protein preparation wizard; to add hydrogen and optimize the protonation states of Thr310 and Ser478 and Asp309 residues. Active site of the *CYP19A1* protein was identified using SiteMap tool of Schrödinger package. We further carried out docking studies by means of Glid, with various ligands. Based on glid score, potential ligands were screened and their interaction with *CYP19A1* was identified. The best hits were further screened for Lipinski's rule for drug-likeness and bioactivity scoring properties. Thus, we report two rubivivaxin and rhodethrin compounds that have successfully satisfied all *in silico* parameters, necessitating further *in vitro* and *in vivo* studies.

Keywords: aromatase inhibitors, anticancer drug, breast cancer, molecular docking

Background:

Breast cancer is the most prevailing malignancy among females, and the second most common cause of cancer-related deaths in women in the United States [1]. An estimated 235,030 new cases of invasive breast cancer are diagnosed among both males and females in the US during 2014 with an estimated death of 40,430 people [2]. Breast cancer is a complex and heterogeneous disease with varying clinical outcomes, disease progression, and responses to specific treatments attributed by a wide array of elements ranging from tumor intrinsic genetic factors to extrinsic

tumor micro-environmental factors [3]. Gene expression studies using DNA microarrays have identified several distinct breast cancer subtypes based on an intrinsic gene list that includes 496 genes that differentiate breast cancers into separate groups based only on gene expression patterns [4]. Estrogens are important players in breast cancer tumorigenesis. The estrogen-bound Estrogen Receptor (ER) complex regulates the transcriptome of breast cancer cells by interaction with different transcription factors. Despite the plethora of physiological and pathophysiological functions of estrogen, a large number of

studies support the role of estrogens in growth and development of ER positive breast cancer [5]. The production of estrogens in human body is mediated by the enzyme Cytochrome P450 aromatase, commonly known as estrogen synthase [6].

Cytochrome P450 aromatase (CYP19A1; EC 1.14.14.1) catalyzes the rate limiting step of estrogen biosynthesis, by the aromatization of C-19 aliphatic androgens to C-18 aromatic estrogens [7, 8]. It is encoded by CYP19A1 gene [9] located on chromosome 15q21.1. The 57.9 kDa molecular weight protein, is made of a single polypeptide chain of 503 amino-acid residues and a prosthetic heme group at its active site [10]. It is widely expressed in many tissues including the gonad of both sexes [11]. In the male gonads, it is generally expressed in the testis and accessory glands wherein it maintains high levels of estradiol needed for normal spermiogenesis, maturation, and motility of sperm [12]. In females, it is mostly expressed in the ovaries of

premenopausal women, and in the placenta of pregnant women. Furthermore, it is also expressed in the peripheral adipose tissues of men and postmenopausal women.

Since ER plays a critical role in breast cancer [13, 14], several therapies have been developed over the past few decades among which endocrine therapy is the foremost treatment for ER positive breast cancer patients [15]. The therapy includes (AIs) aromatase inhibitors, (SERMs) selective estrogen receptor modulators and (SERDs) selective estrogen receptor down regulators. These agents function by either reducing circulating estrogen levels or competing with estrogen for binding to its receptor [16]. AIs bind and block the active site of aromatase thus preventing the conversion of androgens to estrogens. Hence they are widely utilized for inhibition of growth and proliferation of breast cancer cells [17] and serve as first-line therapy for metastatic breast cancer.

Table 1: Induced Fit docking results of drug molecules and reference ligand ASD showing Glide gScore, Glide energy and IFD score with CYP19A1

DrugBank ID	Ligand	Glide gScore (Kcal/mol)	Glide Energy (Kcal/mol)	IFD Score (Kcal/mol)
DB00197	Troglitazone	-13.24	-63.51	-981.61
DB00539	Toremifene (SERM)	-10.97	-52.09	-976.98
DB00894	Testolactone	-10.85	-50.76	-976.54
DB01406	Danazol	-10.88	-60.43	-975.58
Nil	Rubivivaxin	-11.04	-49.96	-975.58
DB01536	Androstenedione (ASD)	-11.06	-50.31	-974.50
DB04839	Cyproterone	-10.32	-47.21	-974.36
DB00882	Clomifene	-10.79	-52.10	-974.21
DB00367	Levonorgestrel	-11.21	-43.14	-974.09
DB00675	Tamoxifen (SERM)	-8.95	-59.11	-974.08
D03784	Liarozole hydrochloride	-10.54	-50.28	-973.99
DB06710	Methyltestosterone	-11.07	-57.21	-973.85
D03749	Plomestane	-9.78	-43.75	-973.17
DB00269	Chlorotrianisene	-10.44	-49.88	-972.83
D03781	Liarozole fumarate	-9.32	-50.27	-972.83
Nil	Rhodethrin	-9.53	-42.34	-972.74
DB00351	Megestrol	-10.75	-52.38	-972.68
DB00255	Diethylstilbestrol	-9.21	-44.85	-972.03
DB01234	Dexamethasone	-11.83	-51.78	-971.93
DB00531	Cyclophosphamide	-6.38	-33.83	-971.68
DB00987	Cytarabine	-8.87	-47.05	-969.89
DB01168	Procarbazine	-7.01	-35.71	-969.90
D02451	Fadrozole hydrochloride	-7.43	-40.94	-969.40
D03778	Fadrozole hydrochloride hydrate	-7.46	-41.70	-969.37
DB01101	Capecitabine	-10.84	-59.63	-968.72
DB00201	Caffeine	-6.20	-33.91	-966.93
Nil	p-Bromophenol	-6.46	-26.26	-966.91
DB00441	Gemcitabine	-6.95	-36.03	-966.63
DB01169	Arsenic trioxide	-3.82	-25.69	-964.89
DB00958	Carboplatin	-5.70	-32.73	-964.89
DB00544	Fluorouracil	-4.36	-14.75	-961.49

Table 2: Molecular Docking Interaction of drug molecules with CYP19A1.^aNumber of hydrogen bonds formed between the CYP19A1 binding domain and the drug compounds. ^bThe interacting active site residues of CYP19A1 protein with the drug molecules in the ligand-receptor complex.

Ligand-enzyme complex	No. of H-bonds ^a	Interacting residues ^b	Atom of the ligand	Bond length (Å)
Troglitazone-CYP19A1	2	Leu 372	H of NH	1.932
		Met 374	O of C=O	1.654
Toremifene-CYP19A1	Nil	Nil	Nil	Nil
Testolactone-CYP19A1	2	Ash 309	O of C=O	1.689
		Met 374	O of C=O	1.845
Danazol-CYP19A1	2	Ash 309	N of	1.990
		Met 374	O of -OH	2.071
Rubrivaxin-CYP19A1	6	Arg 115	O of -COOH	1.834
		Ala 306	H of -OH	1.906
		Ala 306	H of -OH	1.575
		Thr 310	O of -OH	2.136
		Leu 372	H of -OH	1.773
		Met 374	O of -COOH	1.705
Androstenedione-CYP19A1	2	Ash 309	O of C=O	1.689
		Met 374	O of C=O	1.888
Cyproterone-CYP19A1	2	Met 374	O of C=O	1.710
		Hem 600	H of -OH	
Clomifene-CYP19A1	Nil	Nil	Nil	Nil
Levonorgestrel-CYP19A1	2	Thr 310	H of -OH	1.895
		Met 374	O of C=O	1.635
Tamoxifen-CYP19A1	1	Ash 309	H of N+H	1.687
Liarozole hydrochloride-CYP19A1	2	Leu 477	H of NH	1.771
		Hem 600	H of N+H	
Methyltestosterone-CYP19A1	3	Ala 306	H of -OH	1.958
		Thr 310	O of -OH	1.737
		Met 374	O of C=O	1.759
Plomestane-CYP19A1	1	Met 374	O of C=O	1.976
Chlorotrianisene-CYP19A1	1	Met 374	O of	2.058
Liarozole fumarate-CYP19A1	2	Leu 372	H of NH	1.940
		Ser 478	H of N+H	
Rhodethrin-CYP19A1	3	Thr 310	O of -COOH	1.940
		Leu 477	H of NH	2.011
		Hem 600	H of -OH	2.458
Megestrol-CYP19A1	2	Leu 372	H of -OH	1.938
		Met 374	O of C=O	1.804
Diethylstilbestrol-CYP19A1	2	Glu 302	H of -OH	1.737
		Leu 477	H of -OH	1.548
Dexamethasone-CYP19A1	3	Ash 309	O of -OH	2.193
		Met 374	O of C=O	1.712
		Ser 478	H of -OH	1.805
Cyclophosphamide-CYP19A1	1	Met 374	O of O=P	2.132
		Ala 306	H of -OH	1.870
Cytarabine-CYP19A1	4	Thr 310	O of -OH	1.861
		Leu 372	H of NH2	1.960
		Leu 477	H of NH2	1.907
Procarbazine-CYP19A1	2	Hem 600	N of N+H2	
		Hem 600	N of NH	2.003
Fadrozole hydrochloride-CYP19A1	1	Met 374	N of C=N	1.876
Fadrozole hydrochloride hydrate-CYP19A1	2	Met 374	N of C=N	
		Hem 600	N of N+H	1.961
Capecitabine-CYP19A1	2	Leu 372	H of -OH	2.100
		Met 374	O of	1.859
Caffeine-CYP19A1	1	Met 374	O of C=O	2.011
p-Bromophenol-CYP19A1	2	Arg 115	H of -OH	
		Met 374	O of -OH	2.045
Gemcitabine-CYP19A1	3	Thr 310	H of NH2	2.307
		Met 374	O of -OH	2.081
		Leu 477	H of -OH	1.722
Arsenic trioxide-CYP19A1	2	Arg 115	O of O=As	1.988
		Met 374	O of O=As	1.654
Carboplatin-CYP19A1	1	Met 374	O of C=O	1.911
Fluorouracil-CYP19A1	1	Met 374	N of	2.017

Methodology:

Despite remarkable success of endocrine therapy, resistance toward these therapies has been detected [18, 19]. In particular, long-time exposure of targeted agents leads to development of resistant malignant cells [20]. Moreover aromatase inhibitors increase the risk of cardiovascular diseases and musculoskeletal symptoms like arthralgia, osteoporosis and decreased bone mineral density (BMD) in post-menopausal women [21, 22 & 23]. As a result, there is a need for improved and effective therapies which could increase the rate of patient survival and in turn improve the quality of life. An important solution towards solving this puzzle would be discovery of new inhibitors and assessing the potential of currently utilized drugs for treating diverse kinds of cancer. Consequently, the present study was conducted to search for novel biomolecules *in-silico* which could suppress or inhibit the activity of aromatase enzyme. In this study, we have evaluated various biomolecules by performing molecular docking using Maestro (Schrödinger) [24] focused on novel therapeutic targets may throw light into more molecular targeted therapies that could specifically and potentially bring down for aromatase enzyme inhibitors.

A comparative molecular docking approach was followed to trace out the most potent inhibitors of aromatase enzyme. We have performed the molecular screening to filter out and identify most relevant aromatase inhibitors. The identified and screened inhibitor molecules were then further processed for docking studies. Rhodethrin [32] and rubrivivaxin [33] are produced by purple non sulfur photosynthetic bacterium *Rubrivivax benzoatilyticus* JA2 has biological significance in cancer cell lines. Hence, we chose rhodethrin and rubrivivaxin for the molecular docking studies and comparatively analysed the docking results with those of the most prevalent aromatase inhibitors such as troglitazone, toremifene, testolactone and danazol. Most of the molecular docking analysis was performed using Maestro (Schrödinger).

Selection of docking molecules

A total set of 45 drug molecules were identified by Transfac and KEGG databases which target and metabolize aromatase enzyme. Out of 45 identified drugs, 42 were downloaded from drug bank [25] and KEGG Drug [26] databases for carrying out docking studies. The remaining 3 drugs (p-Bromophenol, rhodethrin and rubrivivaxin) were sketched in ChemDrawUltra 13.0 (<http://www.cambridgesoft.com/EnsembleforChemistry/ChemBio3D/ChemBio3DUltra13.0Suite/Default.aspx>) and saved in MDL molfiles. Subsequently, all the ligands were prepared using LigPrep (Schrödinger) by modifying the torsions of the ligands and assigning them appropriate protonation states (Glide-Schrödinger), a single stereochemical structure was generated per ligand with possible states at target pH 7.0 ± 2.0 using Ionizer and Epik by adding metal binding states, tautomerized, desalted and optimized by producing low energy 3D conformation for the ligand under the Optimized Potentials for Liquid Simulations (OPLS-2005) force field while retaining the specified chiralities of the input ligand.

ISSN 0973-2063 (online) 0973-8894 (print)

327

Bioinformation 12(6): 324-331 (2016)

Preparation of target protein

The molecular structure of human aromatase enzyme (PDB ID: 3S79) was retrieved from Protein Data Bank (PDB) with a resolution of 2.75 Å. Before docking the ligands into the protein's active site, the protein was prepared using Schrödinger's molecular docking software, Maestro9.3. The protein was imported to Maestro, in order to investigate the heme-prosthetic group as binding pocket of the enzyme adopted by a ligand in the binding cleft for depiction of both ligand and receptor was a key importance of all hetero groups using protein preparation wizard. Hydrogen atoms were added to the protein to define correct ionization and tautomeric states of amino acid residues. Finally energy minimization was performed using default constraint of 0.3 Å of Root Mean Square Deviation (RMSD) and OLPS-2005 force field.

Induced Fit Docking (IFD) and Extra Precision (XP) Protocol

IFD and XP were performed using the module IFD of Schrödinger-Maestro v9.3 [19]. Initially Glide docking was carried out for each ligand. The sample ring conformations of ligands were selected and the side chains were trimmed. The prime side chain prediction and minimization was carried out in which residues were refined within 6.0 Å of ligand poses and side chains were optimized. This led to creation of a ligand structure and conformation that is IF to each pose of the receptor structure. Finally, Glide XP redocking was carried out as per default conditions. The ligand was rigorously docked into the induced-fit receptor structure (IFRS) and the results yielded by IFD score for each output pose.

Drug-likeness, total drug-score and toxicity risk of compounds

Calculation for various drug properties, such as mutagenic, tumorigenic, irritant nature and an adverse effect of the compounds on the reproductive system was performed using Molinspiration (<http://www.molinspiration.com/cgi-bin/properties>) and Osiris Property Explorer (<http://www.organic-chemistry.org/prog/peo>). The tools also give the drug-likeness and total drug-score of the compounds based on the "Lipinski rule of five". The overall drug score of a compound is the drug-likeness, i.e. logarithm of the partition coefficient between 1-octanol and water, for the hydrophilicity of the compound, where low log P refers to high absorption or permeation, value less than 5 ($c \log P$) and a unit stripped logarithm (log S) for the aqueous solubility of a compound in mol/L. The molecular weight and toxicity risk were calculated by Osiris Property Explorer (OPE) for each compound, thus having an overall potential to qualify for a drug.

Results:

The purification and crystallization of human *CYP19A1* protein has greatly facilitated the identification of compounds which could inhibit its expression, thus providing therapeutic treatments for ER positive breast cancer patients. Discovery of novel inhibitors is primarily based on computational techniques, among which IFD plays a vital role in understanding the

molecular interaction between ligand and the active site of protein. In view of this, all the ligands were docked into the active site of aromatase enzyme (**Table 1**). The active site of protein is occupied by its natural substrate androstenedione (ASD). It forms H-bonds with backbone residues metal Asp309 (1.689 Å) and Met374 (1.888 Å) (**Figure 1**).

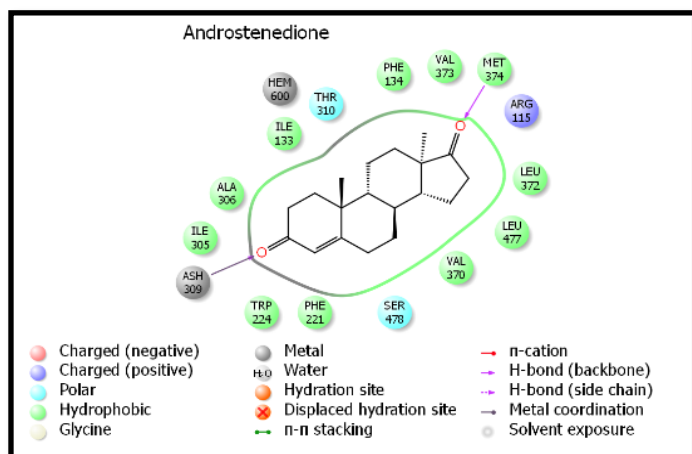


Figure 1: Molecular interaction of natural substrate Androstenedione (ASD) with CYP19A1 protein.

The side chains of residues Thr310 and Ser478 make polar interactions with the bound substrate while positive charge interaction was found with Arg115. The residues Ile133, Phe134, Phe221, Trp224, Ile305, Ala306, Val370, Leu372, Val373 and Leu 477 make hydrophobic interactions with the substrate. The ranking of ligands was based on the IFD score. More negative IFD score indicates better interaction of inhibitor with the target protein (**Table 1**). A Comparison of IFD score of drug molecules with AIs suggested that the drug molecules namely troglitazone, toremifene, testolactone, danazol, rubivivaxin and rhodethrin showed fairly potent activity against CYP19A1 with more negative IFD Score value. Thus, these drug molecules could prove to be more potent than the available third-generation aromatase inhibitors (**Table 2**). To understand the in-depth interaction pattern between the ligands and CYP19A1 protein, Maestro Ligand interaction 2-D diagram was used. The molecules rubivivaxin and rhodethrin shown the drug-likeness and toxicity risk values are less than with troglitazone, toremifene, testolactone, danazol, it indicates that, the molecules has an overall potential to qualify as lead molecules (**Table 3**).

Binding mode of Troglitazone with the ligand binding region of Aromatase

Docking results showed that the ligand troglitazone occupied the ligand binding region of CYP19A1 with an IFD Score of -981.60, Glide gScore of -13.23 and the Glide energy is -63.51 Kcal/mol. Hydrogen bond interactions were identified with the backbone amino acid residues Leu372 and Met374. Twelve hydrophobic interactions with the amino acid residues Ile133, Phe134, Phe221, Trp224, Ile305, Ala306, Ala307, Val369, Val370, Val373, Cys437

and Leu477; one positive charge interaction with Arg115 and two polar interaction with the amino acid residues Thr310 and Ser478 in the ligand binding region of CYP19A1 were observed (**Figure 4**).

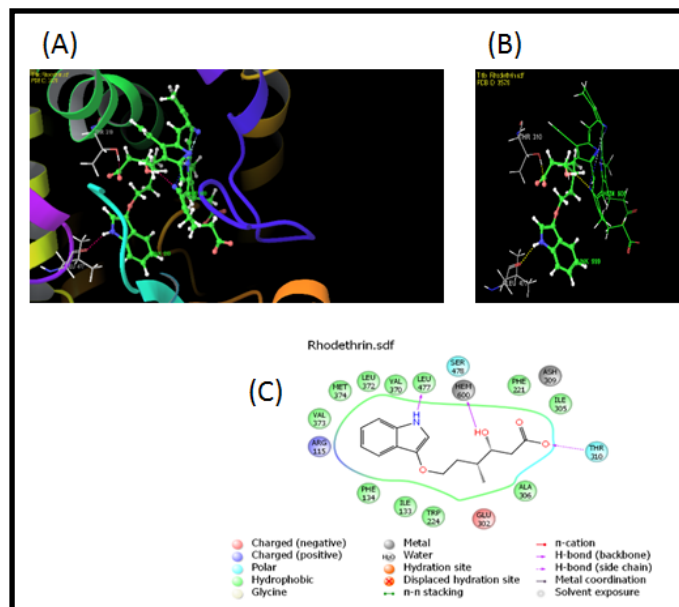


Figure 2: Close view, Binding mode and interacted ligands of Rhodethrin with CYP19A1. A. Close view of Rhodethrin with CYP19A1. B. Binding mode of Rhodethrin with CYP19A1. C. Interaction with ligands.

Binding mode of Toremifene with the ligand binding region of Aromatase

Docking results showed that the ligand toremifene occupied the ligand binding region of CYP19A1 with an IFD Score of -976.97, Glide gScore of -10.97 and the Glide energy is -52.09 Kcal/mol. Trp224 was involved in the π - π stacking interaction with ligand. Sixteen hydrophobic interactions with the amino acid residues Met127, Ile133, Phe134, Phe148, Ile217, Tyr220, Phe221, Met303, Ile305, Ala306, Val369, Val370, Leu372, Val373, Met374 and Leu477; one positive charge interaction with Arg115; one negative charge interaction with Glu302 and two polar interaction with the amino acid residues Thr310 and Ser478 in the ligand binding region of CYP19A1 were observed (**Figure 5**).

Binding mode of Testolactone with the ligand binding region of Aromatase

The ligand testolactone occupied the ligand binding region of CYP19A1 with an IFD Score of -976.54, Glide gScore of -10.85 and the Glide energy is -50.76 Kcal/mol. Hydrogen bond interactions were identified with the backbone amino acid residue Met374 and metal Asp309. Ten hydrophobic interactions with the amino acid residues Ile133, Phe134, Phe221, Trp224, Ile305, Ala306, Val370, Leu372, Val373 and Leu477; one positive charge interaction with Arg115; one negative charge interaction with Glu302 and two polar interaction with the amino acid residues

Thr310 and Ser478 in the ligand binding region of *CYP19A1* were observed (Figure 6).

Table 3: Molinspiration and Osiris results of compounds

Compounds	cLogP	Solubility	Mol. Weight	TPSA	Drug -Likeness	Drug -Score	Toxicity Risk
Troglitazone	4.39	-5.46	441	110.1	3.55	0.47	No Risk
Toremifene	4.95	-4.8	405	12.47	4.33	0.15	High Risk
Testolactone	2.71	-3.74	300	43.37	-2.73	0.43	No Risk
Danazol	3.46	-4.88	337	46.26	2.07	0.62	No Risk
Rubrivivaxin	1.03	-1.78	298	124.2	3.46	0.55	No Risk
Rhodethrin	1.55	-2.62	263	82.55	-1.21	0.56	No Risk

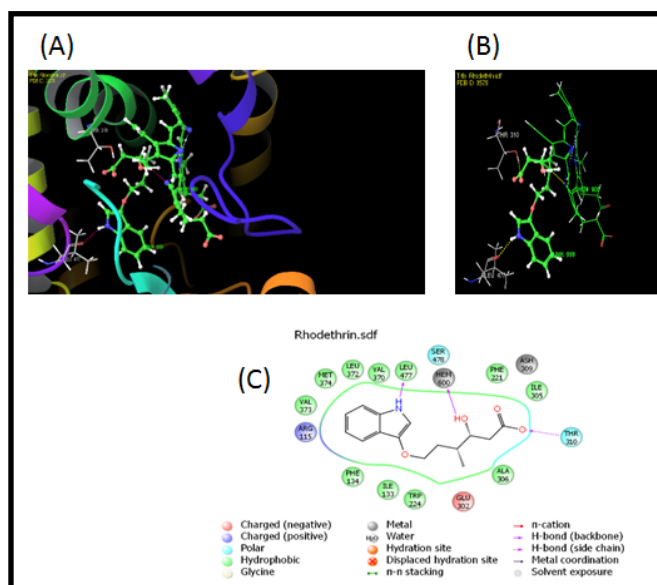


Figure 3: Close view, Binding mode and interacted ligands of Rubrivivaxin with *CYP19A1*. **A.** Close view of Rubrivivaxin with *CYP19A1*. **B.** Binding mode of Rubrivivaxin with *CYP19A1*. **C.** Interaction with ligands

Binding mode of danazol with the ligand binding region of Aromatase

Docking results showed that the ligand danazol occupied the ligand binding region of *CYP19A1* with an IFD Score of -975.58, Glide gScore of -10.88 and the Glide energy is -60.43 Kcal/mol. Hydrogen bond interactions were identified with the backbone amino-acid residue Met374 and metal Ash309. Phe221 was involved in the π - π stacking interaction with ligand. Ten hydrophobic interactions with the amino acid residues Ile133, Phe134, Trp224, Ile305, Ala306, Val370, Leu372, Val 373, Ile398 and Leu477; one positive charge interaction with Arg115 and two polar interactions with the amino acid residues Thr310 and Ser478 in the ligand binding region of *CYP19A1* were observed (Figure 7).

Binding mode of rubrivivaxin with the ligand binding region of Aromatase

The ligand rubrivivaxin occupied the ligand binding region of *CYP19A1* with an IFD Score of -975.58, Glide gScore of -11.04 and

the Glide energy is -49.96Kcal/mol. Hydrogen bond interactions were identified with the backbone amino acid residues Ala306, Leu372, Met374 and side chain amino acid residues Arg115 and Thr310. Ten hydrophobic interactions with the amino acid residues Ile133, Phe134, Phe221, Trp224, Ile305, Ala307, Val370, Val373, Cys437 and Leu477, and one polar interaction with the amino acid residue Ser478 in the ligand binding region of *CYP19A1* were observed (Figure 3).

Binding mode of rhodethrin with the ligand binding region of Aromatase

The ligand rhodethrin occupied the ligand binding region of *CYP19A1* with an IFD Score of -972.74, Glide gScore of -9.53 and the Glide energy is -42.34 Kcal/mol. Hydrogen bond interactions were identified with the backbone amino acid residues Leu477 and Hem600 and side chain amino acid residue Thr310. Eleven hydrophobic interactions with the amino acid residues Ile133, Phe134, Phe221, Trp224, Ile305, Ala306, Val370, Leu372, Val373, Met374, Leu477; one positive charge interaction with Arg115; one negative charge interaction with Glu302 and two polar interaction with the amino acid residue Thr310 and Ser478 in the ligand binding region of *CYP19A1* were observed (Figure 2).

Discussion:

Molecular docking is considered as one of the best methods to identify the protein-ligand interactions during *in silico* phases of drug discovery [27]. Previous studies suggest that aromatase activity can be suppressed in the presence of troglitazone [28], toremifene [29], testolactone [30] and danazol [31]. Hence, we have selected these four different aromatase inhibitors and novel drug targets rubrivivaxin and rhodethrin for our docking studies to comparatively investigate binding efficiency with *CYP19A1*. The results of docking were verified by considering some top clusters of conformations in to the best scored one. The Novel rubrivivaxin and rhodethrin shown the drug-likeness and toxicity risk values are less than with troglitazone, toremifene, testolactone, danazol, it indicates that, the novel drugs has an overall potential to qualify for a drug. The docking results have shown that troglitazone has relatively lesser binding energy followed by rubrivivaxin and toremifene. Thus, our results suggest that the novel compound rubrivivaxin and rhodethrin which are shown a lesser binding energy in comparison with the other molecules may prove potential in structure based drug design to make a major impact on anticancer chemotherapy.

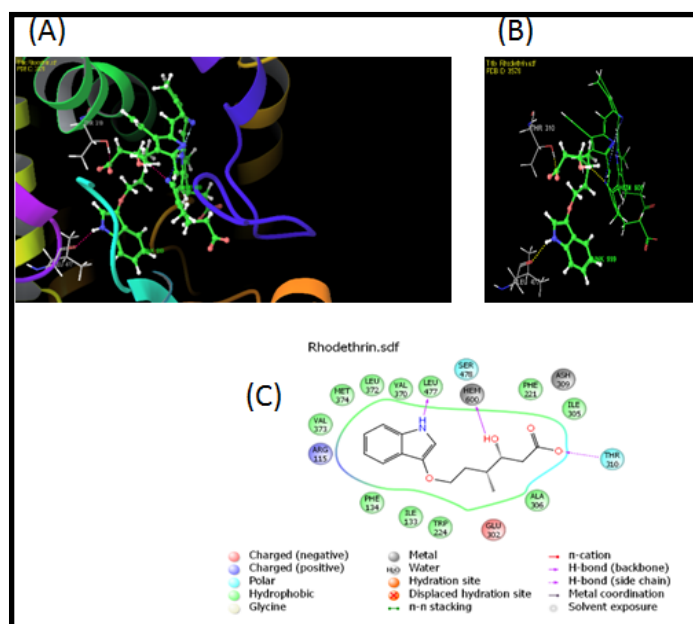


Figure 4: Close view, Binding mode and interacted ligands of Troglitazone with CYP19A1. **A.** Close view of Troglitazone with CYP19A1. **B.** Binding mode of Troglitazone with CYP19A1. **C.** Interaction with ligands.

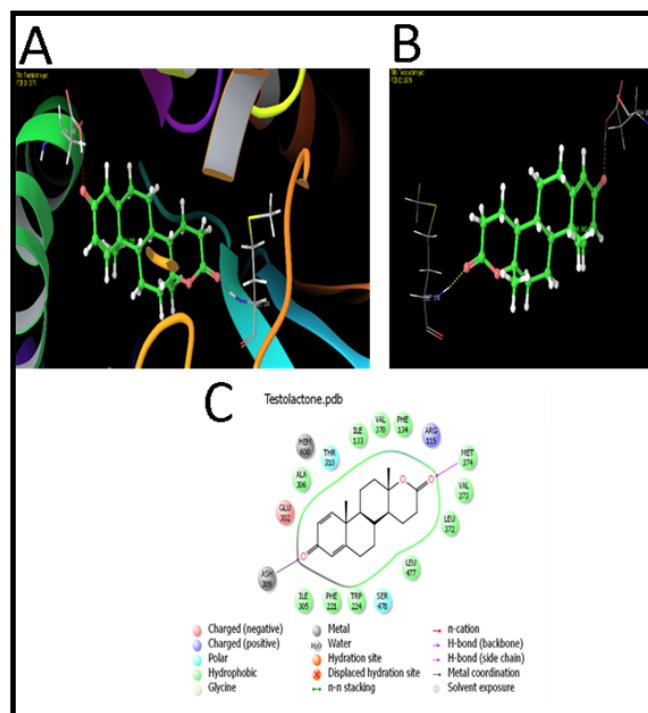


Figure 6: Close view, Binding mode and interacted ligands of Testolactone with CYP19A1. **A.** Close view of Testolactone with CYP19A1. **B.** Binding mode of Testolactone with CYP19A1. **C.** Interaction with ligands.

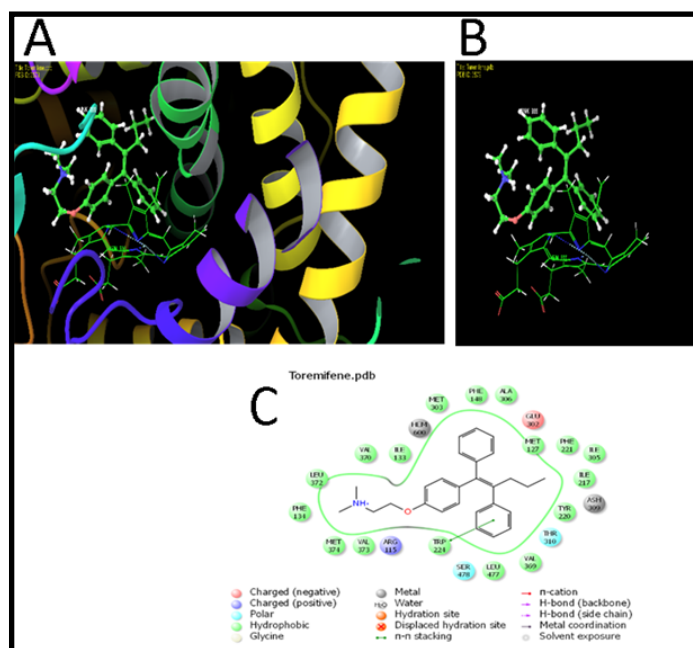


Figure 5: Close view, Binding mode and interacted ligands of Toremifene with CYP19A1. **A.** Close view of Toremifene with CYP19A1. **B.** Binding mode of Toremifene with CYP19A1. **C.** Interaction with ligands 5929.

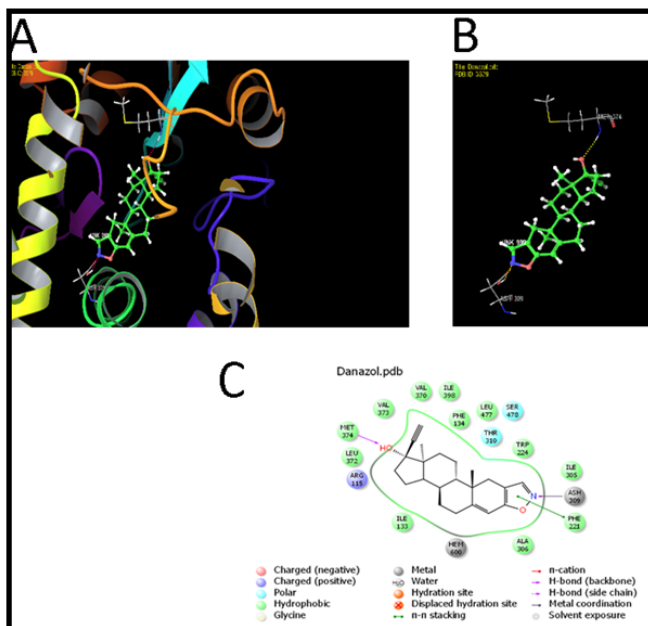


Figure 7: Close view, Binding mode and interacted ligands of Danazol with CYP19A1. **A.** Close view of Danazol with CYP19A1. **B.** Binding mode of Danazol with CYP19A1. **C.** Interaction with ligands.

Conclusion:

Aromatase (*CYP19A1*) is associated with androgenic human breast cancer. Hence, it is important to develop improved inhibitors for Aromatase enzyme. In this study, we described *in silico* docking studies to identify inhibitors and performed to analyze the inhibition of aromatase activity. Two biomolecules namely rubrivivaxin and rhodethrin showed good binding affinity with Aromatase enzyme inhibition. Consequently, the results obtained from this study may be worthwhile, to carry out further *in vitro* and *in vivo* studies to design novel and potential inhibitors against Aromatase (*CYP19A1*).

Acknowledgments:

We are highly thankful to Schrodinger for providing the free version of software to carry out the entire project. Also, we are grateful to Dr. Ravi Kumar Muttineni for his technical assistance at various stages of the project. This work has been supported by DST-SERB, Govt. of India and also APK was supported by grants from National Medical Research Council of Singapore [R-713-000-177-511], the NCIS Yong Siew Yoon Research Grant through donations from the Yong Loo Lin Trust and the National Research Foundation Singapore and the Singapore Ministry of Education under its Research Centers of Excellence initiative to Cancer Science Institute of Singapore, National University of Singapore.

Conflict of interests:

The authors confirmed that this research article content has no conflict of interest.

Reference:

- [1] Jemal *et al.* *CA Cancer J Clin.* 2010 **60**: 277. [PMID: 20610543]
- [2] American Cancer Society, *Cancer Facts & Figures 2014*. Atlanta: American Cancer Society.
- [3] Bertos NR & Park M, *J Clin Invest.* 2011 **121(10)**: 3789. [PMID: 21965335]
- [4] Perou CM *et al.* *Nature.* 2000 **406(6797)**: 747. [PMID: 10963602]
- [5] Marta K & Halina M, *Adv Clin Exp Med.* 2012 **21(4)**: 535. [PMID: 23240460]
- [6] Ackerman GE & Carr BR, *Endocr Metab Disord* 2002 **3**: 225. [PMID: 12215717]
- [7] Simpson *et al.* *Endocr Rev* 1994 **15**: 342. [PMID: 8076586]
- [8] Brueggemeier *et al.* *Endocrine Reviews* 2005 **26(3)**: 331. [PMID: 15814851]
- [9] Sebastian S & Bulun SE, *J. Clin Endocrinol Metab* 2001 **86**: 4600. [PMID: 11600509]
- [10] Suvannang *et al.* *Molecules* 2014 **16**: 3597. [PMID: 26417339]
- [11] Bulun *et al.* *Pharmacol Rev* 2005 **57**: 359. [PMID: 16109840]
- [12] Carreau *et al.* *Adv Med Sci* 2008 **53**: 139. [PMID: 18614433]
- [13] Russo *et al.* *J. Steroid. Biochem. Mol. Biol.* 2003 **87**: 1. [PMID: 14630087]
- [14] Cui *et al.* *J. Clin Oncol.* 2005 **23**: 7721. [PMID: 16234531]
- [15] Rowan TC & Garnet LA, *J Natl Cancer Inst* 2012 **104**: 517. [PMID: 22427684]
- [16] Adam Brufsky M, *Community Oncology* 2011 **8(8)**: 343.
- [17] Altundag K & Ibrahim NK, *The Oncologist* 2006 **11**: 553. [PMID: 16794235]
- [18] Selma *et al.* *J Steroid Biochem. Mol. Bio* 2010 **18(4-5)**: 277.
- [19] Cynthia W & Shuan C, *Journal of Steroid Biochemistry & Molecular Biology* 2012 **131**: 83. [PMID: 22265958]
- [20] Dowsett M *et al.* *J Steroid Biochem Mol Bio* 2005 **195**: 167. [PMID: 15982868]
- [21] Henry *et al.* *Breast Cancer Res Treat* 2008 **111(2)**: 365. [PMID: 17922185]
- [22] Kittaneh & Glück, *Breast Cancer: Basic and Clinical Research* 2011 **5**: 209. [PMID: 22084574]
- [23] Tomao *et al.* *Expert Rev Anticancer Ther* 2011 **11(8)**: 1253. [PMID: 21916579]
- [24] Suite Maestro, version 9.3, Schrödinger, LLC, New York, NY, 2012.
- [25] Wishart DS *et al.* *Nucleic Acids Res* 36. 2008D901. [PMID: 18048412]
- [26] Kanehisa M & Goto S, *Nucleic Acids Res* 2000 **28**: 27. [PMID: 10592173]
- [27] Meng XY *et al.* *Current computer-aided drug design*, 2011 **7(2)**: 146. [PMID: 21534921]
- [28] Brown KA & Simpson ER, *In Obesity and Breast Cancer 2014* (pp. 37-42) Springer, New York, USA
- [29] Ogata H *et al.* *Cancer & chemotherapy* 2013 **40(6)**: 749. [PMID: 23863651]
- [30] Schweikert HU & Tunn UW, *Steroids* 1987 **50(1)**: 191. [PMID: 2460975]
- [31] Murakami K *et al.* *Fertility and sterility* 2006 **86(2)**: 291. [PMID: 16806212]
- [32] Ranjith NK *et al.* *Biotechnol. Lett.* 2007 **29 (9)**: 1399. [PMID: 17636389]
- [33] Kumavath, R.K, *et al.* *World Journal of Microbiology and Biotechnology* 2011 **27**: 11.

Edited by P Kanguane

Citation: Kumavath *et al.* *Bioinformation* 12(6): 324-331 (2016)

License statement: This is an Open Access article which permits unrestricted use, distribution, and reproduction in any medium, provided the original work is properly credited. This is distributed under the terms of the Creative Commons Attribution License.